

Multiscale analysis of multifunctional nanocomposites for aerospace applications

Federica Zaccardi¹

Sapienza Università di Roma, Via Eudossiana 18, 00184 Roma, Italy

Multifunctional nanocomposites based on carbon nanoparticles are promising solution for many technological challenges of the aerospace field. However, the prediction of their properties is still an issue. In this work, carbon-based nanocomposite properties are investigated through a multiscale approach. Starting from the characterization of the single-walled carbon nanotubes (SWCNTs) and matrix properties, the interactions between the SWCNTs and the matrix are studied for a better evaluation of the nanocomposite properties. After the characterization of the interactions, the mechanical and electrical properties of the polymer nanocomposite made of well-dispersed SWCNTs are studied at varying SWCNTs weight fractions and aspect ratios. In the final part, the mechanical and electrical properties of a single-ply plain weave carbon fiber composite are analyzed.

Nomenclature

t_n	=	normal stress, stress component along the local 3-direction in three dimensions
t_s	=	shear stress, stress component along the local 1-direction in three dimensions
t_t	=	shear stress, stress component along the local 2-direction in three dimensions
k_n	=	normal stiffness [N/m ³], stiffness component along the local 3-direction in three dimensions
k_s	=	shear stiffness [N/m ³], stiffness component along the local 1-direction in three dimensions
k_t	=	shear stiffness [N/m ³], stiffness component along the local 2-direction in three dimensions
δ_n	=	separation along the local 3-direction in three dimensions
δ_s	=	separation along the local 1-direction in three dimensions
δ_t	=	separation along the local 2-direction in three dimensions

I. Introduction

Among the nanomaterials, the extraordinary specific mechanical, electrical and thermal properties of carbon nanotubes make them exceptionally suited as reinforcing fillers for polymer composites. They allow an increase of mechanical properties with their high specific stiffness and strength, at the price of a very low weight increase^{1,2}. Moreover, they not only allow an increase in the mechanical properties, but they make possible the realization of multifunctional composites, with enhanced electrical and thermal properties. Therefore, the most interesting aspect is their ability to enhance different properties at the same time, allowing the realization of multifunctional lightweight composites^{2,3}. This opportunity is particularly relevant in the aerospace field⁴, where the use of such materials can satisfy the lightweight requirement by replacing complex and heavier subsystems of a spacecraft.

However, even if lot of efforts are being made to predict the nanocomposites properties, few progresses have been made. In fact, nanocomposites properties depend on many aspects, such as the type of matrix, the type of carbon nanotubes, their functionalization, chirality and aspect ratio, their level of dispersion and/or alignment and their interactions with the matrix³. Taking into account all of these aspects is extremely difficult even if necessary if we want to predict and/or evaluate the final composite properties.

This work tries to overcome these difficulties through a multiscale approach, which can help to address some problems in the prediction of the nanocomposites properties. In fact, it has been widely recognized the necessity for a more systematic approach to the study of nanocomposite materials through multiscale modelling techniques. Multiscale material modelling combines existing and emerging methods, numerical simulations and laboratory

¹ Master student in Space and Astronautical Engineering, federica.zaccardi@gmail.com

experiments, to bridge the wide range of time and length scales which concern a large number of phenomena and processes⁴. Multiscale modelling techniques developed especially in the recent years with the advance of nanotechnology and nanocomposite materials and allow to predict the macroscopic behaviour of the nanocomposite starting from the understanding of its components at the nanoscale/microscale level, to end with a macroscopic understanding of the composite through fem analysis techniques. The link between the two scales is based on the concept of the representative volume element (RVE). At the macroscale level, every point of the body corresponds to the centre of a RVE, which is large enough to adequately represent the heterogeneities at the microscale level, but small with respect to the dimensions of the body⁵.

In fact, even if carbon nanotubes reinforced polymer may look similar to fiber reinforced composites, the scale of carbon fibers and carbon nanotubes (CNTs) is completely different, and continuum mechanics approach fail in predicting the composite properties when nanofillers are used. It is necessary to understand the transferring process of CNTs properties to the whole composite, starting from its characterization at the nanoscale level, and this can be done through multiscale modelling⁶. One of the main differences between a conventional fiber reinforced composite and a nanocomposite is the important role played by the interface between the CNT and the matrix⁶; between them a large interfacial area is available for stress transfer, therefore a primary interest of this work is the characterization of the interface properties between CNTs and the matrix phase.

Therefore, starting from the characterization of the SWCNTs and matrix properties, the interactions between the matrix and the SWCNTs, and between SWCNTs, were studied for a better evaluation of the nanocomposite properties. After the study of these interactions, the properties of a polymer nanocomposite made of well-dispersed SWCNTs were studied at varying aspect ratios and weight fractions. In the final part, the properties of a single-ply plain weave carbon fiber composite were analysed. In particular, the work focuses on the mechanical and electrical properties of the nanocomposites, evaluated through the analysis of RVEs using the software Digimat. In particular, the tool Digimat-FE is used for the prediction of the mechanical properties, while for the evaluation of the electrical properties, both tools Digimat-FE and Digimat-MF were used. Digimat-MF uses mean-field homogenization methods (Mori-Tanaka and Double inclusion methods) to evaluate the properties of RVEs, while Digimat-FE is based on the FEM analysis of RVEs.

II. Interface

For an accurate analysis, it is important to describe the interfacial properties between a nanotube and the polymer matrix. In case of interface between two different material phases in a composite, the main interest is to study the stress transfer across the interface, or, in other words, the properties of the bonding. Usually, to describe the inclusion-matrix debonding at the interface, two approaches can be used: debonding at interface and debonding at inter-phase⁵. The interface is the surface between the inclusion and the matrix, with no thickness; the interphase is the zone of the matrix that is influenced by an inclusion, and it has a finite thickness⁵. At the level of the finite element model, allowing debonding between the inclusions and the matrix is a good way to avoid unreal finite element distortion⁵. Therefore, it can help to solve convergence problems in cases where excessive distortion is observed⁵. The analysis were carried out defining an interface to describe the interactions between the SWCNT's and the matrix. In Digimat-FE the "interface" is referred to the surface (2D) between the inclusion and the matrix. The interface was used instead of the inter-phase because the zone of the matrix influenced by the inclusion is very thin.

A. Cohesive Zone Model

To effectively simulate debonding at interface, the Cohesive Zone Model (CZM) available in Digimat-FE was used. To use the CZM in Digimat-FE, it just has to be defined the cohesive material. At the level of the finite element modelling, debonding is modelled using something very similar to a contact, which is a special surface interaction property⁵. Because of this, it has the same problem of the contact. The most important problem is the convergence, which arise in particular when using second order finite elements⁵; therefore, first order tetrahedral elements were used. The cohesive zone model is typically composed of an elastic part, defined by a traction-separation law, a damage initiation criterion and a damage evolution law. A traction-separation law relates the nominal stress vector to the nominal strain across the cohesive zone. Since the interface has no thickness, it is necessary to work with separations instead of strains. Traction and separation vectors each have three components in 3D, one component normal to the surface (along the local 3-direction, in three dimensions) and two shear components (along the local 1- and 2-directions, in three dimensions). The elastic behaviour can then be written as

$\mathbf{t}=\mathbf{k}\delta$ where \mathbf{t} is the traction stress vector (with components t_n , t_s and t_t), δ is the separation vector (with components δ_n , δ_s and δ_t) and \mathbf{k} is the 3x3 elasticity matrix, whose components have dimensions N/m³ since we are working with separations instead of strains. In Digimat-FE coupled behaviour between the normal and shear components is not supported, therefore the tensile and shear behaviours of the CZM are independent up to failure; this also means that the off-diagonal terms in the elasticity matrix are zero (the only elasticity matrix components are the diagonal terms k_n , k_s and k_t).

As concerns the damage initiation criterion and the damage evolution law, the maximum stress criterion and the damage evolution law based on displacement with linear softening were used, respectively.

Nanotube-matrix interactions

Despite the importance of a univocal method for the description of the interface properties (stiffnesses and ultimate strengths), necessary to understand and describe different phenomena, such as the adhesion or the stress transfer between the nanotubes and the matrix, the problem has not yet been solved. In fact, the interfacial properties depend on many parameters: nanotubes aspect ratio, number of nanotube walls, nanotubes functionalization, type of matrix. Because of all these variables, most of the available data for the description of the interface are specific data for specific cases. Therefore, a method which is general and takes into account all of these variables has not yet been developed. In this work, the objective is to describe the properties of the interface, finding the stiffnesses and the ultimate strengths, between a single-wall carbon nanotube and an epoxy matrix. The thermoset resin considered in this study is the HexFlow RTM6 produced by Hexcel Corporation, which is an epoxy matrix typically used in the aerospace industry. It is composed of the epoxy resin tetraglycidil methylene dianiline (TGMDA) whose chemical formula is C₂₅H₃₀N₂O₄, and the hardeners 4,4'-methylene-bis (2,6-diethylaniline) (MDEA) and 4,4'-methylene-bis (2-isopropyl-6-methylaniline) (M-MIPA), whose chemical formula is the same. The mix ratio between the base resin and the hardeners is 100 parts to 68.2 parts. The density of the cured epoxy is 1140 kg/m³, with an average polymer chain of C_{23.38}H₃₀O_{2.38}N₂.

In nanocomposite structures, the bonding between the nanotubes and the matrix is mainly due to the weak van der Waals interactions⁷. Even though the functionalization of the CNTs can introduce some strong chemical bonds at the interface, in the analysis it was assumed that the only interacting forces between the epoxy matrix and the nanotubes were the van Der Waals forces. The Lennard-Jones (L-J) potential is used to describe the van der Waals interactions at the nanotube/polymer interface. The expression of the van der Waals force between two atoms obtained from the Lennard-Jones potential is:

$$F(r) = 24 \left(\frac{\mu}{\psi} \right) \left[2 \left(\frac{\psi}{r} \right)^{13} - \left(\frac{\psi}{r} \right)^7 \right] \quad (1)$$

Where $F(r)$ is the van der Waals force between two atoms, r is the distance between the atoms, μ is the potential well depth and ψ is the hard sphere radius of the atom or the distance at which the Lennard-Jones potential is zero. The Lennard-jones parameters for the interactions considered are reported in Table 1:

L-J interactions	μ (Joule)	ψ (nanometers)
Carbon-Carbon (C-C)	3.89x10 ⁻²²	0.34
Carbon-Hydrogen (C-H)	4.44x10 ⁻²²	0.32
Carbon-Oxygen (C-O)	4.90x10 ⁻²²	0.32
Carbon-Nitrogen (C-N)	4.48x10 ⁻²²	0.33

The tensile properties of the SWCNT/RTM6 nanocomposite were studied considering only van der Waals interactions between the SWCNT and the polymer matrix. Jiang et al.⁷ established a cohesive law for CNT/polyethylene interfaces based only on the interatomic potential. The expression found by Jiang et al.⁷ was modified to obtain a cohesive law (Eq. (2)) for the SWCNT/RTM6 system considered, where the interactions of the carbon atoms of the SWCNT with the carbon, hydrogen, oxygen and nitrogen atoms of the RTM6 epoxy resin are considered:

$$\begin{aligned}
t_n \cong & \left(2\pi * 23.38 * \rho_p \rho_c \psi_{C-C} \mu_{C-C}^2 \left[\frac{\mu_{C-C}^4}{(\delta_{n,eq} + \delta_n)^4} - \frac{2\mu_{C-C}^{10}}{5(\delta_{n,eq} + \delta_n)^{10}} \right] \right) \\
& + \left(2\pi * 30 * \rho_p \rho_c \psi_{C-H} \mu_{C-H}^2 \left[\frac{\mu_{C-H}^4}{(\delta_{n,eq} + \delta_n)^4} - \frac{2\mu_{C-H}^{10}}{5(\delta_{n,eq} + \delta_n)^{10}} \right] \right) \\
& + \left(2\pi * 2.38 * \rho_p \rho_c \psi_{C-O} \mu_{C-O}^2 \left[\frac{\mu_{C-O}^4}{(\delta_{n,eq} + \delta_n)^4} - \frac{2\mu_{C-O}^{10}}{5(\delta_{n,eq} + \delta_n)^{10}} \right] \right) \\
& + \left(2\pi * 2 * \rho_p \rho_c \psi_{C-N} \mu_{C-N}^2 \left[\frac{\mu_{C-N}^4}{(\delta_{n,eq} + \delta_n)^4} - \frac{2\mu_{C-N}^{10}}{5(\delta_{n,eq} + \delta_n)^{10}} \right] \right)
\end{aligned} \tag{2}$$

Where ρ_p is the polymer volume density (number of polymer molecules per unit volume) and is given by the ratio of the cured epoxy mass density, 1140 kg/m³, to the mass of C_{23.38}H₃₀O_{2.38}N₂ unit; ρ_c is the SWCNT area density (number of carbon atoms per unit area of SWCNT) which equals 3.89x10¹⁹ m⁻² and $\delta_{n,eq}$ is the equilibrium distance between the nanotube and the polymer. In Fig. 1 is represented in red the normal cohesive stress t_n against the interface opening displacement δ_n obtained through Eq. (2), from which the cohesive strength (black point in Fig. 1) $t_n^0 \simeq 717$ MPa occurring at the nominal separation $\delta_n^0 \simeq 0.45$ Å (separation at initiation of damage), the normal stiffness $k_n \simeq 1.4 \times 10^{19}$ N/m³ and the separation at failure $\delta_n^f \simeq 2.6$ Å were derived.

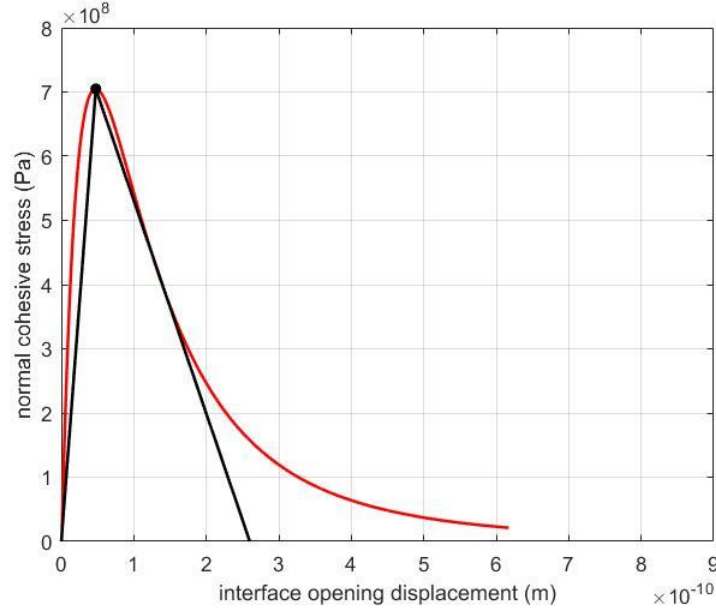


Figure 1. Normal cohesive stress against interface opening displacement. In red is represented the cohesive law for a carbon nanotube and the RTM6 epoxy resin obtained through Eq. (3), considering only van der Waals interactions; in black is represented the corresponding bilinear cohesive law.

As concerns the shear cohesive stress, it was not derived an analytical expression of t_s and t_t as functions of the separations δ_s and δ_t , respectively; therefore, data available in literature were used. In particular, Wernick et al.⁸ found the interfacial shear strength t_s^0 (assumed equal to t_t^0) to be 25 MPa, occurring at a sliding distance of $\delta_s^0 \simeq 1$ nm (assumed equal to δ_t^0), and therefore $k_s=k_t \simeq 2.4 \times 10^{16}$ N/m³. As concerns the values of the separations at failure δ_s^f and δ_t^f , it was assumed that the difference between the separations at failure (δ_s^f and δ_t^f) and the separations at initiation of damage (δ_s^0 and δ_t^0) are the same and equal to the difference between δ_n^f and δ_n^0 ($\simeq 2.15$ Å, as it can be seen from Fig. 1)

Nanotube-nanotube interactions

Also the nanotube-nanotube interactions were analyzed. In all of the analysis that were carried out, it was made the hypothesis of perfectly distributed carbon nanotubes, which means that it is supposed the absence of SWCNTs clusters in the nanocomposite, and therefore a minimum distance among SWCNTs was imposed. Lu et al.⁹ established a cohesive law for CNT walls in multi-wall CNTs, which is here supposed to be the same between two CNTs. The profile of the cohesive force per unit of length against the opening displacement is represented in Fig. 2. In Digimat, in all of the RVEs analyzed, the distance at which the cohesive force (per unit of length) reaches 1% of its maximum value was set as the minimum distance among SWCNTs in the RVEs. This minimum distance is about 1.1 nm. The value that the cohesive force per unit of length assumes at this minimum distance is indicated with a blue point in Fig. 2. With a black point is indicated the maximum cohesive force per unit of length, which is about 6.8×10^3 N/m.

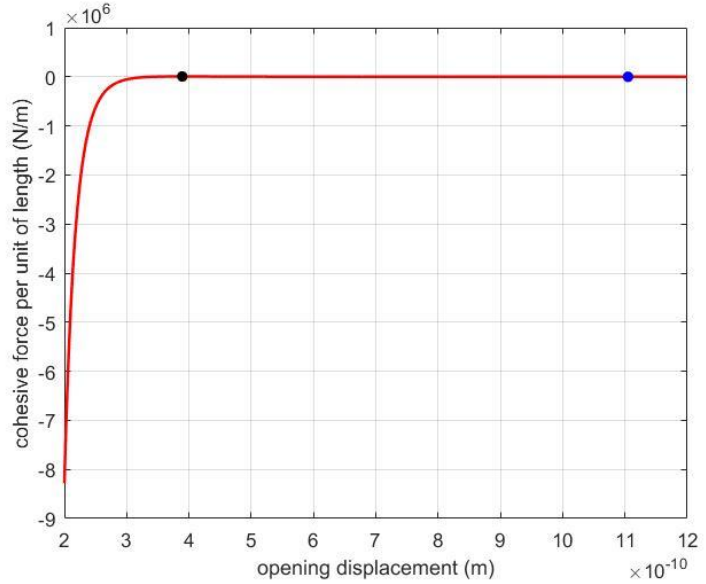


Figure 2. Normal cohesive force per unit of length against the opening displacement. In red is represented the cohesive force per unit of length between two CNT walls.

III. Materials

The materials considered in the analysis are single wall carbon nanotubes, epoxy resin, and carbon fibers. The SWCNTs are assumed to have a Young's modulus¹⁰, Poisson's ratio¹⁰ and maximum strain¹⁰ of, respectively, 1TPa, 0.3 and 0.15. The density¹¹ and the shear strength¹² were assumed to be, respectively, 1350 Kg/m³ and 60 GPa, while the tensile strength, under the hypothesis of isotropic elastic behaviour, was evaluated as 150 GPa, which is a little higher than the values usually obtained with molecular dynamics (MD) simulations¹³, but realistic¹⁴. SWCNTs not only have exceptional mechanical properties, but also a high electrical conductivity, around $10^6/10^7$ S/m. A value of 0.5×10^7 was considered in this work. As concerns the epoxy resin, the HexFlow RTM6 produced by the Hexcel Corporation was considered, assuming a shear strength^{15,16} of 40 MPa, and an electrical conductivity of 10^{-10} S/m (dielectric material). Both the SWCNTs and the RTM6 epoxy resin were supposed to be isotropic materials with linear elastic behaviour until breakage. The carbon fibers taken into account are the Toray T300 produced by the Toray company; they were modelled as transversely isotropic¹⁷, with linear elastic behaviour until breakage.

IV. SWCNT/RTM6 nanocomposite

In this paragraph are discussed the mechanical and electrical properties of the SWCNT/RTM6 nanocomposite evaluated at the microscale level through non-linear quasi-static FEM analysis of adequate RVEs at varying SWCNTs weight fractions (w.f.) and aspect ratios (AR). In all of the analysis, it was made the hypothesis of randomly and perfectly distributed SWCNTs, therefore in all of the RVEs analyzed a random placement of SWCNTs and a minimum distance of 1.1 nm among SWCNTs were imposed.

A. Mechanical analysis

The first set of analysis carried out with Digimat-FE are the mechanical analysis. The SWCNTs were represented as sphero-cylinders with constant diameter of 2 nm. A random placement and a minimum distance of 1.1 nm among SWCNTs were imposed in all the RVEs analysed.

RVEs with constant SWCNTs aspect ratio and weight fraction

A first set of analysis with SWCNTs weight fraction of 0.5% and aspect ratio of 5 was carried out. In Fig. 3(a) is represented the geometry of the RVE and in Fig. 3(b) the meshed geometry. As concerns the RVE size (an isotropic behavior of the RVE is expected when a certain RVE size is reached), convergence of the analysis was reached with a number of 10 SWCNTs (RVE size: $0.04 \times 0.04 \times 0.04 \mu\text{m}^3$); as concerns the mesh, convergence of the analysis was reached with 170000 finite elements, with finite elements size varying from $0.001 \mu\text{m}^3$ to $0.0002 \mu\text{m}^3$. In fact, by increasing the RVE size or by using a finer mesh the results of the post-process analysis did not changed. The loadings were applied one at a time, and the difference between the bonded and non-bonded (when the CZM is applied at the interface) cases is analyzed. At first, a uniaxial loading in the x-direction and a shear loading in the x-y plane were applied and it can be seen from the stress-strain curves that when the interface debonding is allowed, the mechanical properties are a little inferior (Fig. 4(a) and Fig. 4(b)). The properties of the nanocomposite with SWCNTs weight fraction of 0.5% and SWCNTs aspect ratio of 5 are summarized in Table 2, where E_y is the Young modulus, G is the shear modulus, σ_u is the tensile strength and τ_u is the shear strength. The results in Table 2 show little differences in the mechanical properties between the bonded and non-bonded cases. In Fig. 5(a) and 5(b) it can be seen the isotropic behaviour of the nanocomposite RVEs: the stress-strain curves obtained when the interface is defined, by applying uniaxial loadings in the x,y or z directions, and the stress-strain curves obtained by applying shear loadings in the x-y, x-z and y-z planes are overlapped.

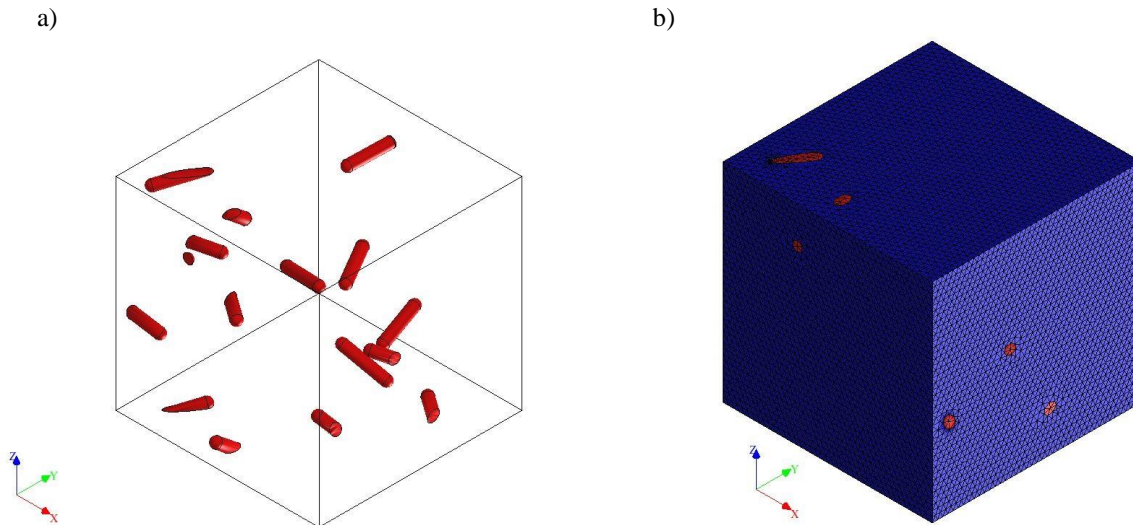


Figure 3. Geometry (a) and mesh (b) of the RVE with SWCNTs weight fraction of 0.5% and SWCNTs aspect ratio of 5.

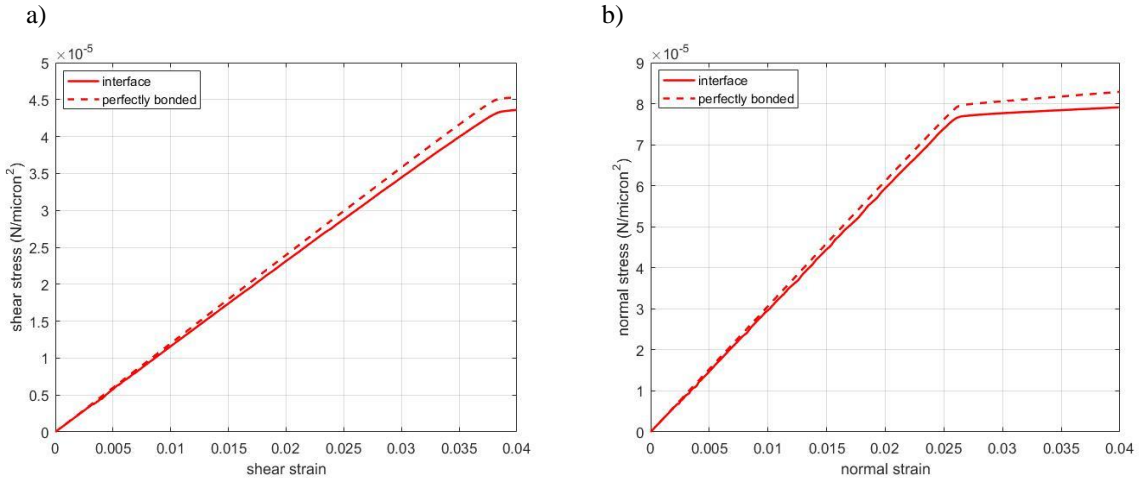


Figure 4. stress-strain curves for a uniaxial loading in the x-direction (a) and a shear loading in the x-y plane (b) applied to an RVE with ten inclusions (SWCNTs), 0.5% SWCNTs weight fraction and SWCNTs aspect ratio=5, in case of perfectly bonded phases and when the interface is defined.

Table 2

0.5% w.f.	σ_u (MPa)	τ_u (MPa)	E_y (GPa)	G (GPa)
Interface	76.60	43.71	3	1.16
Perfectly bonded	79.21	44.92	3.06	1.19

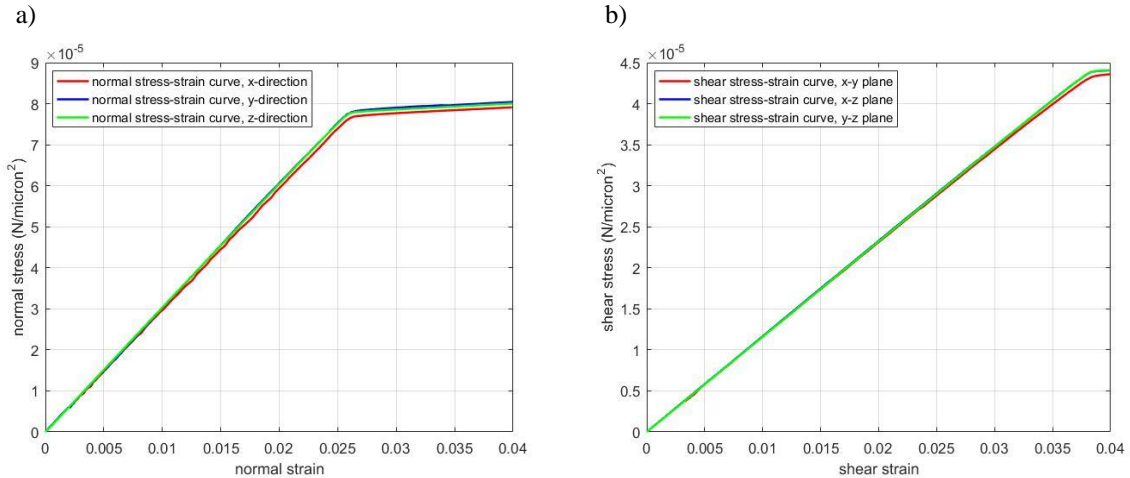


Figure 5. Stress-strain curves when uniaxial loadings in the x, y and z-directions are applied (a) and stress-strain curves when shear loadings in the x-y, x-z and y-z planes are applied (b) to an RVE with ten inclusions (SWCNTs), 0.5% SWCNTs weight fraction and SWCNTs aspect ratio=5, when the interface is defined. The curves in (a) and in (b) are almost overlapped.

RVEs with constant SWCNTs aspect ratio and varying weight fraction

RVEs with 1% and 2% SWCNTs weight fractions were analyzed. The results obtained following the same approach of the previous paragraph are summarized in Table 3 and Table 4. In this case it is observed a significant difference between the bonded and non-bonded cases. When the interface is defined, the properties evaluated are similar to those present in current literature¹⁸; the same cannot be said when the properties are evaluated considering perfectly bonded matrix (RTM6) and inclusion (SWCNTs) phases, that leads to significantly higher (and incorrect) mechanical properties, thus proving the importance of the characterization and definition of the interface for a correct evaluation of the nanocomposite properties. Moreover, by increasing the weight fraction from 0.5% to 1%, a significant improvement in the mechanical properties is observed. The same cannot be said when the weight fraction is increased from 1% to 2%, with the mechanical properties which remains basically the same. Therefore, it can be said that 1% w.f. represents an optimum value from a mechanical point of view, allowing the realization of nanocomposites with increased mechanical properties, at the price of low weight increase. Moreover, the results were found by making the hypothesis of perfect SWCNTs dispersion (no clusters), which can be a strong assumption when considering high SWCNTs weight fractions (e.g. 2% w.f.).

Table 3

1% w.f.	σ_u (MPa)	τ_u (MPa)	E_y (GPa)	G (GPa)
Interface	83.95	47.59	3.21	1.26
Perfectly bonded	92.24	49.11	3.51	1.33

Table 4

2% w.f.	σ_u (MPa)	τ_u (MPa)	E_y (GPa)	G (GPa)
Interface	85.9	46.57	3.24	1.26
Perfectly bonded	96.58	51.09	3.56	1.33

RVEs with varying SWCNTs aspect ratio and constant weight fraction

In this paragraph the results of the analysis of RVEs at varying SWCNTs aspect ratios are discussed. The hypothesis and the procedure followed are the same of the previous analysis. The SWCNTs weight fraction was kept constant to 0.5% and the values of the SWCNTs aspect ratio considered were 5, 15, 25 and 55. As it can be observed from Fig. 6 where are represented the stress-strain curves obtained in case of uniaxial loading in the x-direction applied to RVEs with different SWCNTs aspect ratio, there is no difference in the mechanical properties for different values of aspect ratios. Overlapped curves were obtained also when uniaxial loadings in the y and z-directions and shear loadings in the x-y, x-z and y-z planes were applied. Therefore, there is no effect of the aspect ratio on the mechanical properties of the nanocomposite. It has to be specified that the maximum value of aspect ratio considered was 55 since higher values led to convergence difficulties of the FEM analysis; therefore the possible effect of higher values of aspect ratios on the mechanical properties was not studied.

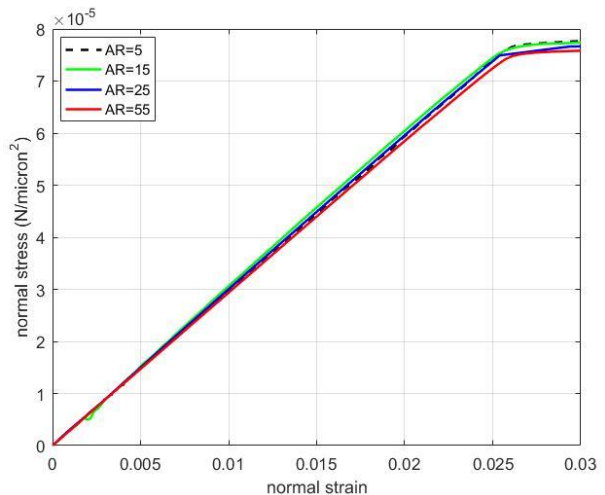


Figure 6. Stress-strain curves when a uniaxial loading in the x-direction is applied to RVEs with SWCNTs of different aspect ratio values.

B. Electrical analysis

After the evaluation of the mechanical properties, the electrical conductivity of the SWCNT/RTM6 nanocomposite was evaluated using Digimat-MF. Again, it was made the hypothesis of randomly and perfectly distributed SWCNTs. The electrical properties of a nanocomposite strongly depend on the CNTs volume fraction, shape, aspect ratio and level of clusterization. In fact, an important phenomenon which might or not occur is the percolation phenomenon, which occurs with conductive inclusions. In particular, the electrical conductivity of the composite strongly depends on the inclusion volume fraction; for low volume fractions, the electrical conductivity is low (essentially equal to the matrix electrical conductivity, which is usually a dielectric material). Then, when the volume fraction reaches a certain value, called the percolation threshold, the conductivity increases by several orders of magnitude, since inclusions are close enough to be in electrical contact. In Digimat-MF it is implemented the following percolation law:

$$\sigma_c = \sigma_{inclusion} \left(\frac{\varphi - \varphi_c}{1 - \varphi_c} \right)^t \quad (3)$$

Where σ_c is the electrical conductivity of the composite, $\sigma_{inclusion}$ is the electrical conductivity of the inclusion (SWCNT in this case), φ is the inclusions volume fraction, φ_c is the percolation threshold and t is the percolation exponent. As concerns the percolation exponent¹⁹, it was assumed that $t \approx 1.96$. As concerns the percolation threshold, the expression proposed by Li et al.²⁰ was considered, where it was assumed a perfect carbon nanotubes dispersion (no clusters) and an aspect ratio of 55. With this assumptions $\varphi_c \approx 7 \times 10^{-3}$. The results of the analysis are listed in Table 5. When the SWCNTs weight fraction is 0.5%, the electrical conductivity is low and basically that of the matrix, since percolation did not occur. When the weight fraction is increased up to 1%, the percolation phenomenon occurs and the electrical conductivity is increased of several orders of magnitude. The results found for the 0.5% and 1% SWCNTs weight fractions, are compatible with the experimental results present in current literature^{21,22}. As concerns the value of the electrical conductivity found for the 2% SWCNTs weight fraction, it is significantly higher than the experimental values. This is explained by the fact that in the analysis it was made the hypothesis of perfect SWCNTs dispersion (no clusters), which is a strong assumption. In real systems, clusterization always occurs and can be a significant aspect when evaluating the properties of nanocomposites. From the results obtained, 1% w.f. represents again an optimum value, which allows the realization of low weight nanocomposites with increased electrical conductivity (and mechanical properties).

Table 5

	RTM6	RTM6 + 0.5% w.f	RTM6 + 1% w.f.	RTM6 + 2% w.f.
σ_c [S/m]	10^{-10}	$2.16 \cdot 10^{-9}$	10.8	204.22

V. Plain weave carbon fiber composite

After the evaluation of the mechanical and electrical properties of SWCNT/RTM6 nanocomposite, at the mesoscale level the properties of a single-ply plain weave carbon fiber composite were evaluated through the analysis of adequate RVEs. In particular, two cases are compared: the case in which the matrix phase is the neat RTM6 epoxy resin and the case in which the matrix phase is the SWCNT/RTM6 nanocomposite at established SWCNTs weight fraction and aspect ratio. In particular, the weight fraction and aspect ratio considered are 1% (optimum value from the mechanical and electrical point of views, with the made assumptions) and 55, respectively; therefore, the properties evaluated in the previous section (IV) were considered for the second case analysis. In Digimat, the definition of an interface between the fiber and the matrix phases is not allowed, therefore a perfect bonding between the two phases was automatically supposed. In Fig. 7(a) is represented the geometry of the RVE analyzed, and in Fig. 7(b) is represented the meshed geometry. As concerns the RVE size (a transversely isotropic behavior of the RVE is expected when a certain RVE size is reached), convergence of the analysis was reached with an RVE size of $8 \times 8 \times 0.77$ mm³; as concerns the mesh, convergence of the analysis was reached with 250000 finite elements. The carbon fibers volume fraction of the analyzed RVE is about 60%. The results found for

the two cases analyzed are shown in Table 6 and Table 7, where E_i are the young moduli, G_{ij} are the shear moduli, ν_{ij} are the Poisson's ratios and σ_i are the electrical conductivities. In this case, both the mechanical and the electrical analysis were performed using Digimat-FE.

As it can be seen from the results in Table 6 and Table 7, the mechanical properties are basically the same for the two cases analyzed, and close to values that can be found in literature²³. As concerns the electrical properties, a significant increase of the electrical conductivity in the z-direction is observed when the matrix phase is the SWCNT/RTM6 nanocomposite. Therefore, by adding 1% SWCNTs weight fraction, it is possible the realization of multifunctional composites with both high mechanical and electrical properties.

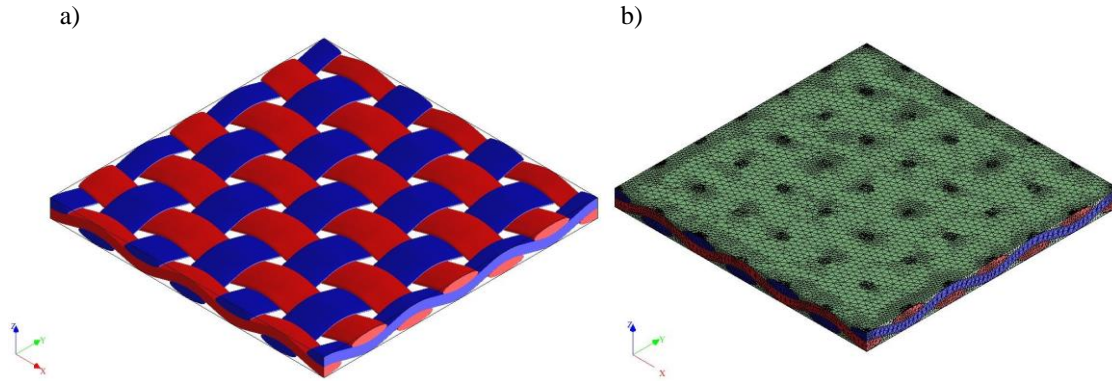


Figure 8. Geometry (a) and mesh (b) of the RVE of the one-ply plain weave carbon fiber composite.

Table 6

	E_x/E_y (GPa)	E_z (GPa)	G_{xy} (GPa)	G_{yz}/G_{xz} (GPa)	ν_{xy}	ν_{xz}/ν_{yz}
RTM6	64	8.07	11.83	5.86	0.032	0.5
RTM6 + 1% SWCNT	64.32	8.43	12	6.1	0.032	0.49

Table 7

	σ_x/σ_y [S/m]	σ_z [S/m]
RTM6	$1.92 \cdot 10^4$	$5.26 \cdot 10^{-6}$
RTM6 + 1% SWCNT	$2.7 \cdot 10^4$	57.14

VI. Conclusion

The multiscale method implemented is based on the analysis of RVEs with perfectly and randomly dispersed carbon nanotubes. The nanotube-matrix and nanotube-nanotube interactions were taken into account for a better prediction of the nanocomposites properties, evaluated at varying nanotube weight fractions and aspect ratios. In particular, only the van der Waals interactions were taken into account, assuming that the only interacting forces between the SWCNTs and the matrix, and among SWCNTs, are the van der Waals forces; this assumption is widely used in molecular dynamic simulations which aim at predicting the interface properties between CNTs and polymer matrices; anyway, further studies could take into consideration the strong interactions which eventually occur between CNTs and the polymer matrix. However, the results of the analysis obtained both at the microscale level with the evaluation of the SWCNT/RTM6 nanocomposite properties, and at the mesoscale level with the evaluation of the single-ply plain weave carbon fiber composite properties, are in good agreement with results that can be found

in current literature, proving the importance of the interface in determining the mechanical properties of the nanocomposites and the validity of the multiscale method proposed (as well as the hypothesis that were made) for the evaluation of the nanocomposites properties.

Acknowledgments

I would like to thank Prof. Laurenzi for the continuous guidance and support. I also acknowledge support from e-Xstream engineering – MSC Software Company for the software Digimat.

References

- ¹Coleman, J. N., Khan, U., Blau, W. J., Gun'ko, Y. K., "Small but strong: A review of the mechanical properties of carbon nanotube-polymer composites", *Carbon*, Vol. 44, No. 9, Aug. 2006, pp. 1624-1652.
- ²Esawi, A. M. K., Farag, M. M., "Carbon nanotube reinforced composites: Potential and current challenges", *Materials & Design*, Vol. 28, No. 9, 2007, pp. 2394- 2401.
- ³Pandey, G., Thostenson, E. T., "Carbon nanotube-based multifunctional polymer nanocomposites", *Polymer Reviews*, Vol. 52, No. 3, 2012, pp. 355-416.
- ⁴Gates, T. S., Odegard, G. M., Frankland, S. J. V., Clancy, T. C., "Computational materials: Multi-scale modeling and simulation of nanostructured materials", *Composites Science and Technology*, Vol. 65, No. 15-16, Dec. 2005, pp. 2416-2434.
- ⁵Digimat 2017.0, Digimat 2017.0 - User's Manual, Software Package Docs, Ver. 2017.0, MSC Software Corporation, 2017.
- ⁶Hasan, Z., "Multiscale analysis of nanocomposites and their use in structural level applications", Ph.D. Dissertation, Arizona State University, Phoenix, AZ, Aug. 2014.
- ⁷Jiang, L. Y., Huang, Y., Jiang, H., Ravichandran, G., Gao, H., Hwang, K. C., Liu, B., "A cohesive law for carbon nanotube/polymer interfaces based on the van der Waals force", *Journal of the Mechanics and Physics of Solids*, Vol. 54, No. 11, Nov. 2006, pp. 2436-22452.
- ⁸Wernik, J.M., Cornwell-Mott, B.J., Meguid, S.A., "Determination of the interfacial properties of carbon nanotube reinforced polymer composites using atomistic-based continuum model", *International Journal of Solids and Structures*, Vol. 49, No. 13, 15 Jun. 2012, pp. 1852-1863.
- ⁹Lu, W. B., Wu, J., Jiang, L. Y., Huang, Y., Hwang K. C., Liu, B., "A cohesive law for multi-wall carbon nanotubes", *Philosophical Magazine*, Vol. 87, No. 14-15, 22 Jun. 2007, pp. 2221-2232.
- ¹⁰Dereli, G., Süngü, B., "Temperature dependence of the tensile properties of single-walled carbon nanotubes: O(N) tight binding molecular-dynamics simulations", *Physical Review B*, Vol. 75, No. 18, 14 May 2007, pp. 184104 .
- ¹¹Collins, P. G., Avouris, P., "Nanotubes for electronics", *Scientific American*, Vol. 283, 2000, pp. 62-69.
- ¹²Min, K., Aluru, N. R., "Mechanical properties of graphene under shear deformation", *Applied Physics Letters*, Vol. 98, No. 1, Jan. 2011, pp. 013113.
- ¹³Rao, P. S., Anandatheertha, S., Naik, G. N., Gopalakrishnan, S., "Estimation of mechanical properties of single wall carbon nanotubes using molecular mechanics approach", *Sadhana*, Vol. 40, No. 4, Jun. 2015, pp. 1301-1311.
- ¹⁴Wagner, H. D., "Nanotube-polymer adhesion: a mechanics approach", *Chemical Physics Letter*, Vol. 361, No. 1-2, 24 Jul. 2002, pp. 57-61.
- ¹⁵Inglis, H. M., Geubelle, P. H., Matouš, K., "Boundary condition effects on multiscale analysis of damage localization", *Philosophical Magazine*, Vol. 88, No. 16, 26 Sep. 2008, pp. 2373-2397.
- ¹⁶Gilat, A., Goldberg, R. K., Roberts, G. D., "Strain Rate Sensitivity of Epoxy Resin in Tensile and Shear Loading", *Journal of Aerospace Engineering*, Vol. 20, No. 2, Apr. 2007, pp. 75-89.
- ¹⁷Miyagawa, H., Mase, T., Sato, C., Drown, E., Drzal, L. T., Ikegami, K., "Comparison of experimental and theoretical transverse elastic modulus of carbon fibers", *Carbon*, Vol. 44, No. 10, Aug. 2006, pp. 2002-2008.
- ¹⁸Gojny, F. H., Wichmann, M. H. G., Köpke, U., Fiedler, B., Schulte, K., "Carbon nanotube-reinforced epoxy-composites: enhanced stiffness and fracture toughness at low nanotube content", *Composites Science and Technology*, Vol. 64, No. 15, Nov. 2004, pp. 2363-2371.
- ¹⁹Hu, L., Hecht, D. S., Grüner, G., "Percolation in transparent and conducting carbon nanotube networks", *Nano Letters*, Vol. 4, No. 12, 22 Oct. 2004, pp. 2513-2517.
- ²⁰Li, J., Ma, P. C., Chow, W. S., To, C. K., Tang, B. Z., Kim, J.-K., "Correlations between Percolation Threshold, Dispersion State, and Aspect Ratio of Carbon Nanotubes", *Advanced Functional Materials*, Vol. 17, No. 16, 2007, pp. 3207-3215.
- ²¹Bai, J. B., Allaoui, A., "Effect of the length and the aggregate size of MWNTs on the improvement efficiency of the mechanical and electrical properties of nanocomposites—experimental investigation", *Composites Part A: Applied Science and Manufacturing*, Vol. 34, No. 8, Aug. 2003, pp. 689-694.
- ²²Sandler, J. K. W., Kirk, J. E., Kinloch, I. A., Shaffer, M. S. P., Windle, A. H., "Ultra-low electrical percolation threshold in carbon-nanotube-epoxy composites", *Polymer*, Vol. 44, No. 19, Sep. 2003, pp. 5893-5899.
- ²³Zhang, Y. C., Harding, J., "A numerical micromechanics analysis of the mechanical properties of a plain weave composite", *Computers and Structures*, Vol. 36, No. 5, 1990, pp. 839-844.